Status of three-neutrino oscillation parameters, circa 2013

F. Capozzi,[1,2] G. L. Fogli,[1,2] E. Lisi,[2] A. Marrone,[1,2] D. Montanino,[3,4] and A. Palazzo[5]

[1]*Dipartimento Interateneo di Fisica "Michelangelo Merlin," Via Amendola 173, 70126 Bari, Italy*
[2]*Istituto Nazionale di Fisica Nucleare, Sezione di Bari, Via Orabona 4, 70126 Bari, Italy*
[3]*Dipartimento di Matematica e Fisica "Ennio De Giorgi," Via Arnesano, 73100 Lecce, Italy*
[4]*Istituto Nazionale di Fisica Nucleare, Sezione di Lecce, Via Arnesano, 73100 Lecce, Italy*
[5]*Max-Planck-Institut für Physik (Werner Heisenberg Institut), Föhringer Ring 6, 80805 München, Germany*

(Received 15 December 2013; published 22 May 2014)

The standard three-neutrino (3ν) oscillation framework is being increasingly refined by results coming from different sets of experiments, using neutrinos from solar, atmospheric, accelerator and reactor sources. At present, each of the known oscillation parameters [the two squared mass gaps $(\delta m^2, \Delta m^2)$ and the three mixing angles $(\theta_{12}, \theta_{13}, \theta_{23})$] is dominantly determined by a single class of experiments. Conversely, the unknown parameters (the mass hierarchy, the θ_{23} octant and the CP-violating phase δ) can currently be constrained only through a combined analysis of various (eventually all) classes of experiments. In the light of recent new results coming from reactor and accelerator experiments, and of their interplay with solar and atmospheric data, we update the estimated $N\sigma$ ranges of the known 3ν parameters and revisit the status of the unknown ones. Concerning the hierarchy, no significant difference emerges between normal and inverted mass ordering. A slight overall preference is found for θ_{23} in the first octant and for nonzero CP violation with $\sin\delta < 0$; however, for both parameters, such preference exceeds 1σ only for normal hierarchy. We also discuss the correlations and stability of the oscillation parameters within different combinations of data sets.

DOI: 10.1103/PhysRevD.89.093018 PACS numbers: 14.60.Pq, 13.15.+g, 11.30.Er

I. INTRODUCTION

The vast majority of experimental results on neutrino flavor oscillations converge towards a simple three-neutrino (3ν) framework, where the flavor states $\nu_\alpha = (\nu_e, \nu_\mu, \nu_\tau)$ mix with the massive states $\nu_i = (\nu_1, \nu_3, \nu_3)$ via three mixing angles $(\theta_{12}, \theta_{13}, \theta_{23})$ and a possible CP-violating phase δ [1]. The observed oscillation frequencies are governed by two independent differences between the squared masses m_i^2, which can be defined as $\delta m^2 = m_2^2 - m_1^2 > 0$ and $\Delta m^2 = m_3^2 - (m_1^2 + m_2^2)/2$, where $\Delta m^2 > 0$ and < 0 correspond to normal hierarchy (NH) and inverted hierarchy (IH), respectively [2]. At present, we know five oscillation parameters, each one with an accuracy largely dominated by a specific class of experiments, namely θ_{12} by solar data; θ_{13} by short-baseline (SBL) reactor data; θ_{23} by atmospheric data, mainly from Super-Kamiokande (SK); δm^2 by long-baseline reactor data from KamLAND (KL); and Δm^2 by long-baseline (LBL) accelerator data, mainly from MINOS and T2K. However, the available data are not yet able to determine the mass hierarchy, to discriminate the θ_{23} octant, or to discover CP-violating effects. A worldwide research program is underway to address such open questions and the related experimental and theoretical issues [3].

In this context, global neutrino data analyses [4–7] may be useful to get the most restrictive bounds on the known parameters, via the synergic combination of results from different classes of oscillation searches. At the same time, such analyses may provide some guidance about the unknown oscillation parameters, a successful example being represented by the hints of $\sin^2\theta_{13} \sim 0.02$ [8–11], which were discussed before the discovery of $\theta_{13} > 0$ at reactors [12–14]. Given the increasing interest in the known oscillation parameters, as well as in possible hints about the unknown ones, we find it useful to revisit the previous analysis in Ref. [4] by including new relevant data which have become available recently (2013–2014) and which turn out to have an interesting impact on the fit results.

In particular, with respect to Ref. [4], we include the recent SBL reactor data from Daya Bay [15] and RENO [16], which reduce significantly the range of θ_{13}. We also include the latest appearance and disappearance event spectra published in 2013 and at the beginning of 2014 by the LBL accelerator experiments T2K [17–19] and MINOS [20,21], which not only constrain the known parameters $(\Delta m^2, \theta_{23}, \theta_{13})$ but, in combination with other data, provide some guidance on the θ_{23} octant and on leptonic CP violation. To this regard, we find a slight overall preference for $\theta_{23} < \pi/4$ and for nonzero CP violation with $\sin\delta < 0$; however, for both parameters, such hints exceed 1σ only for normal hierarchy. No significant preference emerges for normal versus inverted hierarchy. Among the various fit results which can be of interest, we find it useful to report both the preferred $N\sigma$ ranges of each oscillation parameter and the covariance plots of selected couples of parameters, as well as to discuss their stability and the role of different data sets in the global analysis.

Our work is structured as follows: In Sec. II we discuss some methodological issues concerning the analysis of different data sets and their combination. In Secs. III and IV we present, respectively, the updated ranges on single oscillation parameters and the covariances between selected couples of parameters. We pay particular attention to the (in)stability and (in)significance of various hints about unknown parameters, also in comparison with other recent (partial or global) data analyses. Finally, we summarize our work in Sec. V.

II. METHODOLOGY

In this section, we briefly discuss the various data sets used and how they are combined in the global fit.

A. LBL accelerator + solar + KL data

Concerning LBL accelerator data, we include the observed energy spectra of events, in both appearance (muon-to-electron flavor) and disappearance (muon-to-muon flavor) oscillation modes, as presented by the T2K [17–19] and MINOS [20–23] experiments. The theoretical spectra are calculated through a suitably modified version of the GLoBES software package [24,25]. We have verified that our fits reproduce very well the regions allowed at various C.L.'s in Refs. [17,18,20–23], under the same restrictive assumptions made therein on specific oscillation parameters (e.g., by limiting their range or fixing them *a priori*). However, we emphasize that no restrictions are applied in the global fit discussed in the next section, where all the 3ν parameters are free to float.

At the current level of accuracy, LBL accelerator data (disappearance plus appearance) are known to be sensitive not only to the dominant parameters $(\pm\Delta m^2, \theta_{23}, \theta_{13})$, but also to the subdominant parameters (δm^2, θ_{12}) and δ. For this reason, as argued in Ref. [4], it is convenient to analyze LBL accelerator data in combination with solar and KL data, which provide the necessary input for (δm^2, θ_{12}). We remark that "Solar + KL" data (here treated as in Ref. [4]) provide a preference for $\sin^2\theta_{13} \sim 0.02$ in our analysis, which plays a role in the combination "LBL Acc. + Solar + KL," as discussed in the next section.

B. Adding SBL reactor data

After the recent T2K observation of electron flavor appearance, the combination of LBL Acc. + Solar + KL data can provide a highly significant measurement of θ_{13} which, however, is somewhat correlated with two unknowns affecting LBL data: the CP violating phase δ and the θ_{23} octant. It is thus important to add the accurate and (δ, θ_{23})-independent measurement of θ_{13} coming from SBL reactor experiments, within a "LBL Acc. + Solar + KL + SBL Reac." combination. In this work, SBL reactor neutrino data are statistically treated as in Ref. [26], with the further inclusion of the most recent data from Daya Bay [15] and RENO [16].

C. Adding atmospheric neutrino data

In this work, the analysis of SK atmospheric neutrino data (phases I–IV) [27–29] is essentially unchanged with respect to Ref. [4]. We remind the reader that such data involve a very rich oscillation phenomenology, which is sensitive, in principle, also to subleading effects related to the mass hierarchy, the θ_{23} octant and the CP phase δ [30]. However, within the current experimental and theoretical uncertainties, it remains difficult to disentangle and probe such small effects at a level exceeding $\sim 1\sigma - 2\sigma$ [2]. Moreover, independent 3ν fits of SK I–IV data [4,6,29] converge on some but not all the hints about subleading effects, as discussed later. Therefore, as also argued in Ref. [4], we prefer to add these data only in the final "LBL Acc. + Solar + KL + SBL Reac. + SK Atm." combination, in order to separately gauge their effects on the various 3ν parameters.

D. Conventions for allowed regions

In each of the above combined data analyses, the six oscillation parameters $(\Delta m^2, \delta m^2, \theta_{12}, \theta_{13}, \theta_{23}, \delta)$ are left free at fixed hierarchy (either normal or inverted). Parameter ranges at N standard deviations are defined through $N\sigma = \sqrt{\chi^2 - \chi^2_{\rm min}}$. As in Ref. [4], this definition is maintained also in plots involving two parameters, where it is understood that the previous $N\sigma$ ranges are reproduced by projecting the two-dimensional contours over one parameter axis [1]. It is also understood that, in each figure, all undisplayed parameters are marginalized away.

Finally, we shall also report the relative preference of the data for either NH or IH, as measured by the quantity $\Delta\chi^2_{\rm I\text{-}N} = \chi^2_{\rm min}({\rm IH}) - \chi^2_{\rm min}({\rm NH})$. This quantity cannot immediately be translated into "$N\sigma$" by taking the square root of its absolute value, because it refers to two discrete hypotheses, not connected by variations of a physical parameter. We shall not enter into the current debate about the statistical interpretation of $\Delta\chi^2_{\rm I\text{-}N}$ [31–33] because, as shown in the next section, its numerical values are not yet significant enough to warrant a dedicated discussion.

III. RANGES OF OSCILLATION PARAMETERS

In this section, we graphically report the results of our global analysis of increasingly rich data sets, grouped in accordance to the previous discussion.

Figures 1, 2 and 3 show the $N\sigma$ curves for the data sets defined in Secs. II A, II B and II C, respectively. In each figure, the solid (dashed) curves refer to NH (IH); however, only the NH curve is shown for the δm^2 and θ_{12} parameters, since the very tiny effects related to the NH-IH difference [4,34] are unobservable in the fit. (Also note that the δm^2 and θ_{12} constraints change very little in Figs. 1–3.) For each

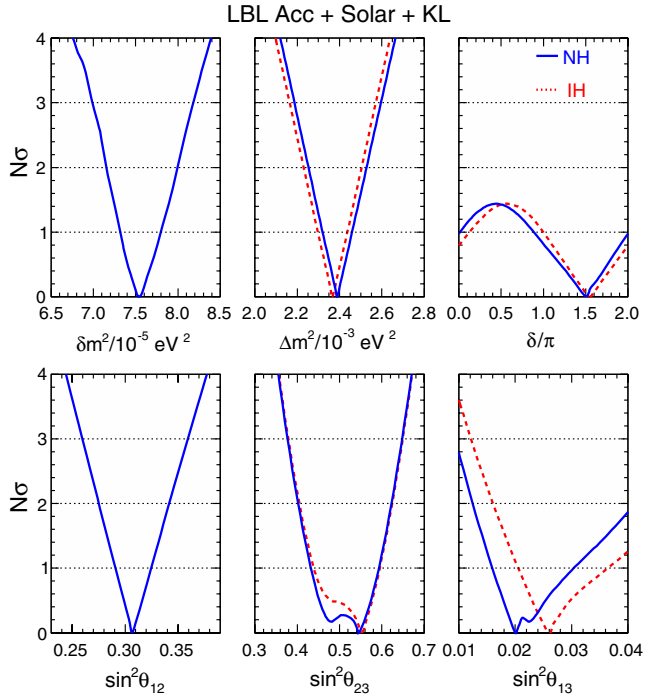

FIG. 1 (color online). Combined 3ν analysis of LBL Acc. + Solar + KL data: Bounds on the oscillation parameters are given in terms of standard deviations $N\sigma$ from the best fit. Solid (dashed) lines refer to NH (IH). The horizontal dotted lines mark the 1σ, 2σ and 3σ levels for each parameter (all the others being marginalized away). See the text for details.

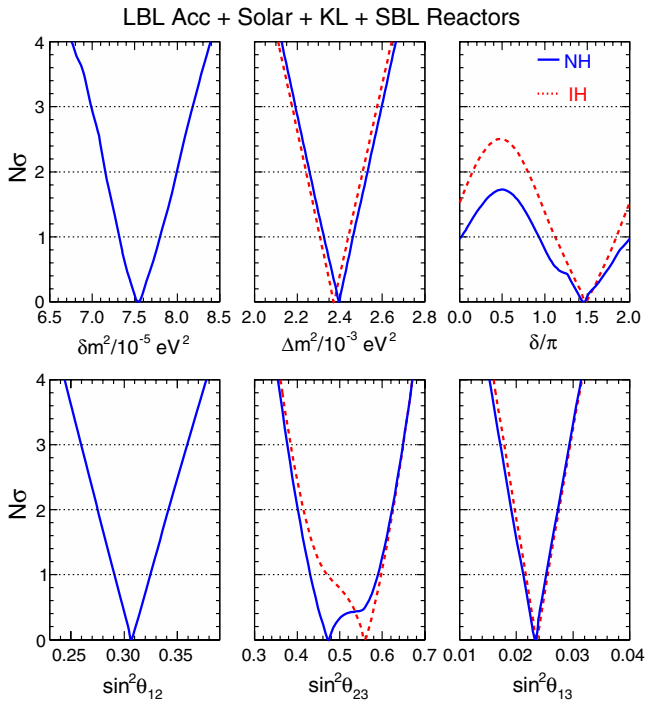

FIG. 2 (color online). As in Fig. 1, but adding SBL reactor data.

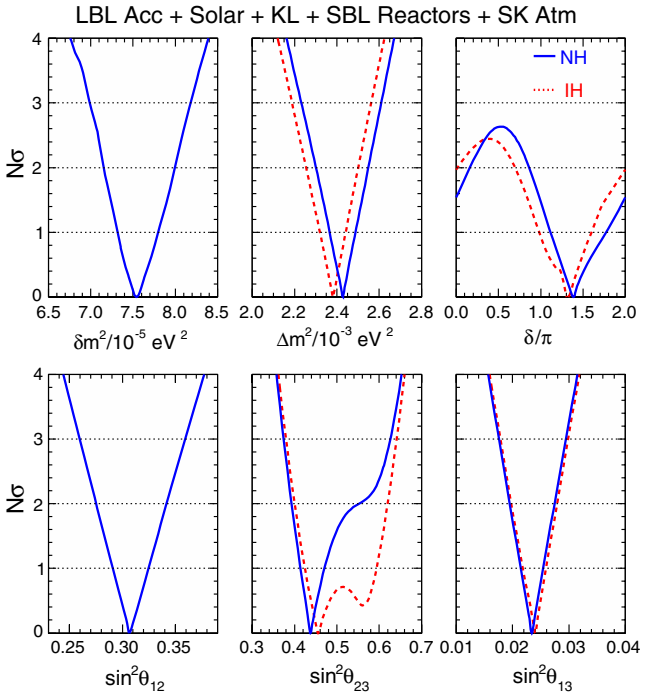

FIG. 3 (color online). As in Fig. 2, but adding SK atmospheric data in a global 3ν analysis of all data.

parameter in Figs. 1–3, the more linear and symmetrical the curves, the more Gaussian is the probability distribution associated with that parameter.

Figure 1 refers to the combination LBL Acc. + Solar + KL, which already sets (without the need of atmospheric and reactor data) highly significant lower and upper bounds on all the oscillation parameters, except for δ. In this figure, the relatively strong appearance signal in T2K [17] plays an important role: it dominates the lower bound on θ_{13}, and it also drives the slight but intriguing preference for $\delta \simeq 1.5\pi$, since for $\sin\delta \sim -1$ the CP-odd term in the $\nu_\mu \to \nu_e$ appearance probability [35,36] is maximized [17]. This trend wins over the current MINOS preference for $\sin\delta \gtrsim 0$ [20,23], since the T2K appearance signal is stronger than the MINOS one and dominates in the global fit. On the other hand, MINOS disappearance data [21,23] still lead to a slight preference for nonmaximal θ_{23}, as compared with nearly maximal θ_{23} in the T2K data fit [18,19]. The (even slighter) preference for the second θ_{23} octant is due to the interplay of LBL accelerator and Solar + KL data, as discussed in the next section.

Figure 2 shows the results obtained by adding (with respect to Fig. 1) the SBL reactor data, whose primary effect is a strong reduction of the θ_{13} uncertainty. Secondary effects include (i) a slightly more pronounced preference for $\delta \simeq 1.5\pi$ and $\sin\delta < 0$, and (ii) a swap of the preferred θ_{23} octant with the hierarchy ($\theta_{23} < \pi/4$ in NH and $\theta_{23} > \pi/4$ in IH). These features will be interpreted in terms of parameter covariances in the next section.

Figure 3 shows the results obtained by adding (with respect to Fig. 2) the SK atmospheric data in the most complete data set. It thus represents a synopsis of the current constraints on each oscillation parameter, according to our global 3ν analysis. The main differences with respect to Fig. 2 include (i) an even more pronounced preference for $\sin\delta < 0$, with a slightly lower best fit at $\delta \simeq 1.4\pi$; (ii) a slight reduction of the errors on Δm^2 and a relatively larger variation of its best-fit value with the hierarchy; and (iii) a preference for θ_{23} in the first octant for both NH and IH, which is a persisting feature of our analyses [2,4]. The effects (ii) and (iii) show that atmospheric neutrino data have the potential to probe subleading hierarchy effects, although they do not yet emerge in a stable or significant way. Concerning effect (i), it should be noted that the existing full 3ν analyses of atmospheric data [6,29], as well as this work, consistently show that such data prefer δ around 1.5π or slightly below, although with still large uncertainties. Table I summarizes in numerical form the results shown in Fig. 3.

When comparing Figs. 1–3, it is interesting to note an increasingly pronounced preference for nonzero CP violation with increasingly rich data sets, although the two CP-conserving cases ($\delta = 0, \pi$) remain allowed at $\lesssim 2\sigma$ in both NH and IH, even when all data are combined (see Fig. 3). It is worth noticing that the two maximally CP-violating cases ($\sin\delta = \pm 1$) have opposite likelihood: while the range around $\delta \sim 1.5\pi\,(\sin\delta \sim -1)$ is consistently preferred, small ranges around $\delta \sim 0.5\pi\,(\sin\delta \sim +1)$ appear to be disfavored (at $> 2\sigma$ in Fig. 3). In particular, for the specific case of NH and at ~90% C.L. ($\sim 1.6\sigma$), only the range $\sin\delta < 0$ is allowed in Fig. 3, while the complementary one is disfavored, with the two CP-conserving cases being just "borderline." In the next few years, the appearance channel in LBL accelerator experiments will provide crucial data to investigate these intriguing CP violation hints.

From the comparison of Figs. 1–3, one can also notice a slight overall preference for nonmaximal mixing ($\theta_{23} \neq 0$), although it appears to be weaker than in Ref. [4], essentially because the most recent T2K data prefer nearly maximal mixing [18,19], and thus they "dilute" the opposite preference coming from MINOS [21,23] and atmospheric data [4]. Moreover, the indications about the octant appear to be somewhat unstable in different combinations of data. In the present analysis, only atmospheric data consistently prefer the first octant in both hierarchies, but the global fit significance is non-negligible (~90% C.L.) only in NH (see Fig. 3). By excluding LBL accelerator data from the global fit, the significance of $\theta_{23} < \pi/4$ would rise to $\sim 2\sigma$ in NH and $\sim 1.5\sigma$ in IH (not shown). It should be noted that, in a recent 3ν global fit [6], the preferred octant toggles with the hierarchy, while in the latest atmospheric 3ν analyses from the SK Collaboration [28,29] (without LBL accelerator data), the second octant is preferred in both NH and IH. We remark that such differences in the θ_{23} fit results should not be considered as conflicting with each other, since they are all compatible within the (still large) quoted uncertainties.

We also emphasize that no atmospheric ν analysis performed outside the SK Collaboration [4–7] can possibly reproduce in detail the official SK one, which currently includes hundreds of bins and > 150 systematic error sources [27]; on the other hand, this level of complexity also hinders the interpretation of subleading effects at the $\sim 1\sigma$ level, such as those related to (non)maximal mixing, which are diluted over many data points and whose size is comparable to systematic uncertainties. We continue to argue, as discussed in Ref. [2], that our slight preference for $\theta_{23} < \pi/4$ in atmospheric ν data stems from a small but persisting overall excess of low-energy electronlike events; see also Ref. [5] for a similar discussion. We are unable to trace the source of a slight preference for $\theta_{23} > \pi/4$ in the official SK analysis. In any case, these fluctuations in atmospheric fit results show how difficult it is to reduce the allowed range of θ_{23} on the basis of atmospheric neutrino data only. In this context, the disappearance channel in LBL

TABLE I. Results of the global 3ν oscillation analysis, in terms of best-fit values and allowed 1σ, 2σ and 3σ ranges for the 3ν mass-mixing parameters. See also Fig. 3 for a graphical representation of the results. We remind that Δm^2 is defined herein as $m_3^2 - (m_1^2 + m_2^2)/2$, with $+\Delta m^2$ for NH and $-\Delta m^2$ for IH. The CP-violating phase is taken in the (cyclic) interval $\delta/\pi \in [0, 2]$. The overall χ^2 difference between IH and NH is insignificant ($\Delta\chi^2_{\text{I-N}} = -0.3$).

Parameter	Best fit	1σ range	2σ range	3σ range
$\delta m^2/10^{-5}\text{eV}^2$ (NH or IH)	7.54	7.32–7.80	7.15–8.00	6.99–8.18
$\sin^2\theta_{12}/10^{-1}$ (NH or IH)	3.08	2.91–3.25	2.75–3.42	2.59–3.59
$\Delta m^2/10^{-3}\text{eV}^2$ (NH)	2.43	2.37–2.49	2.30–2.55	2.23–2.61
$\Delta m^2/10^{-3}\text{eV}^2$ (IH)	2.38	2.32–2.44	2.25–2.50	2.19–2.56
$\sin^2\theta_{13}/10^{-2}$ (NH)	2.34	2.15–2.54	1.95–2.74	1.76–2.95
$\sin^2\theta_{13}/10^{-2}$ (IH)	2.40	2.18–2.59	1.98–2.79	1.78–2.98
$\sin^2\theta_{23}/10^{-1}$ (NH)	4.37	4.14–4.70	3.93–5.52	3.74–6.26
$\sin^2\theta_{23}/10^{-1}$ (IH)	4.55	4.24–5.94	4.00–6.20	3.80–6.41
δ/π (NH)	1.39	1.12–1.77	$0.00 - 0.16 \oplus 0.86 - 2.00$	⋯
δ/π (IH)	1.31	0.98–1.60	$0.00 - 0.02 \oplus 0.70 - 2.00$	⋯

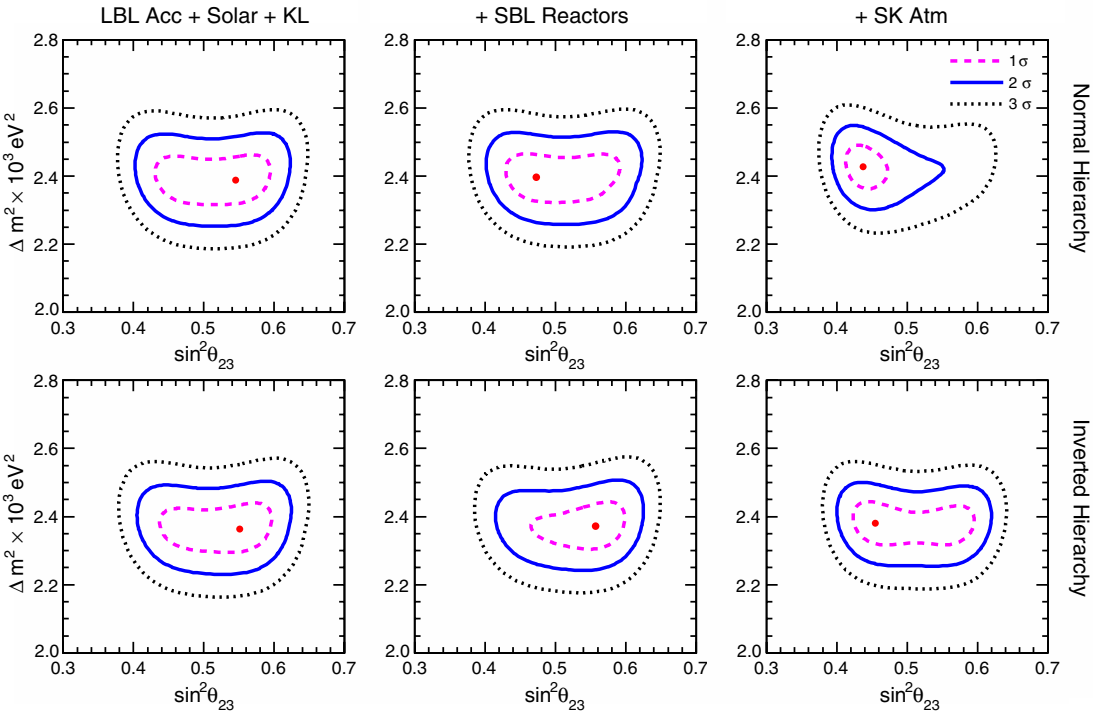

FIG. 4 (color online). Results of the analysis in the plane charted by ($\sin^2\theta_{23}$, Δm^2), all other parameters being marginalized away. From left to right, the regions allowed at 1σ, 2σ and 3σ refer to increasingly rich data sets: LBL accelerator + solar + KamLAND data (left panels), plus SBL reactor data (middle panels), plus SK atmospheric data (right panels). Best fits are marked by dots. The three upper (lower) panels refer to normal (inverted) hierarchy.

accelerator experiments will provide independent and increasingly accurate data to address the issue of nonmaximal θ_{23} in the next few years.

Finally, we comment on the size of $\Delta\chi^2_{\text{I-N}}$ which, by construction, is not apparent in Figs. 1–3. We find $\Delta\chi^2_{\text{I-N}} = -1.4, -1.1, -0.3$ for the data sets in Figs. 1, 2, and 3, respectively. Such values are both small and decreasing with increasingly rich data sets; thus, they do not provide us with relevant indications about the hierarchy.

IV. COVARIANCES OF OSCILLATION PARAMETERS

In this section, we show the allowed regions for selected couples of oscillation parameters and discuss some interesting correlations.

Figure 4 shows the global fit results in the plane charted by ($\sin^2\theta_{23}$, Δm^2), in terms of regions allowed at 1σ, 2σ and 3σ ($\Delta\chi^2 = 1, 4$ and 9). Best fits are marked by dots, and it is understood that all the other parameters are marginalized away. From left to right, the panels refer to increasingly rich data sets, as previously discussed: LBL accelerator + solar + KamLAND data (left), plus SBL reactor data (middle), plus SK atmospheric data (right). The upper (lower) panels refer to normal (inverted) hierarchy. This figure shows the instability of the θ_{23} octant discussed above, in a graphical format which is perhaps more familiar to most readers. It is worth noticing the increasing ($\sin^2\theta_{23}$, Δm^2) covariance for increasingly nonmaximal θ_{23} (both in the first and in the second octant), which contributes to the overall Δm^2 uncertainty. In this context, the measurement of Δm^2 at SBL reactor experiments (although not yet competitive with accelerator and atmospheric experiments [15]) may become relevant in the future: being θ_{23} independent, it will help to break the current correlation with θ_{23} and to improve the overall Δm^2 accuracy in the global fit.

Figure 5 shows the allowed regions in the plane charted by ($\sin^2\theta_{23}$, $\sin^2\theta_{13}$). Let us consider first the left panels, where a slight negative correlation between these two parameters emerges from LBL appearance data, as discussed in Ref. [4]. The contours extend towards relatively large values of θ_{13}, especially in IH, in order to accommodate the relatively strong T2K appearance signal [17]. However, solar + KL data provide independent (although weaker) constraints on θ_{13} and, in particular, prefer $\sin^2\theta_{13} \sim 0.02$ in our analysis. This value, being on the "low side" of the allowed regions of θ_{13}, leads (via anticorrelation) to a best-fit value of θ_{23} on the "high side" (i.e., in the second octant) for both NH and IH. However, when current SBL reactor data are included in the middle panels, a slightly higher value of θ_{13} is preferred ($\sin^2\theta_{13} \simeq 0.023$) with very small uncertainties: this value is high enough to flip the θ_{23} best fit from the second to the first octant in NH, but not in IH.

It is useful to compare the left and middle panels of Fig. 5 with the analogous ones of Fig. 1 from our previous

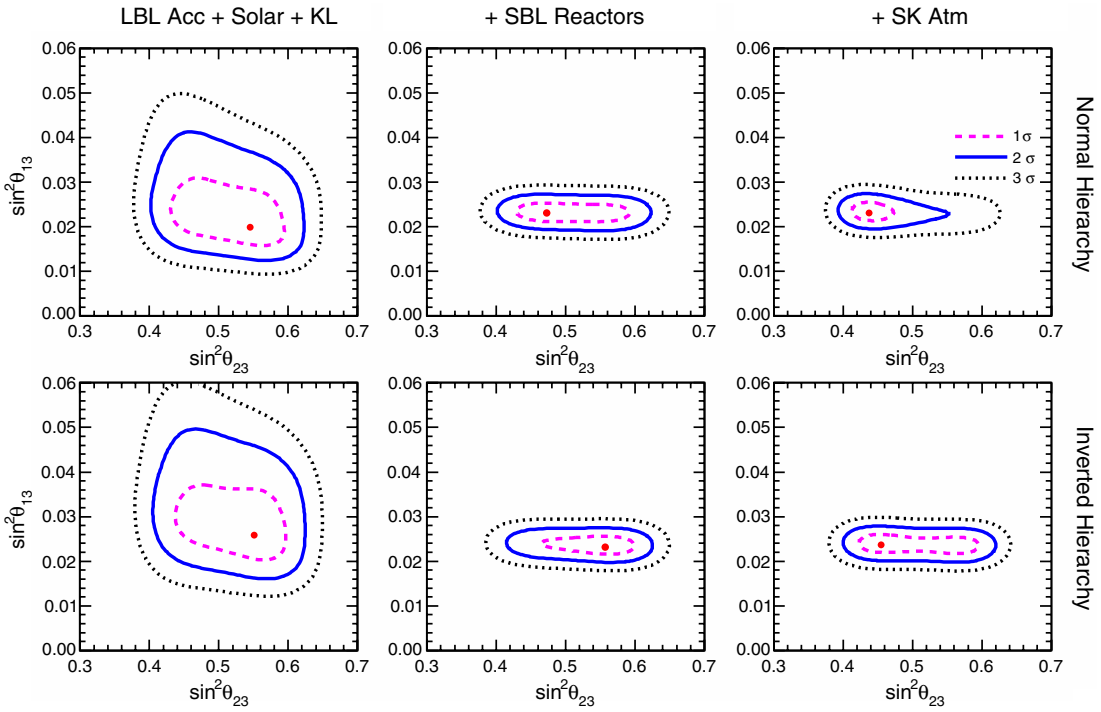

FIG. 5 (color online). As in Fig. 4, but in the plane ($\sin^2\theta_{23}$, $\sin^2\theta_{13}$).

analysis [4]: the local minima in the two θ_{23} octants are now closer and more degenerate. This fact is mainly due to the persisting preference of T2K disappearance data for nearly maximal mixing [19], which is gradually diluting the MINOS preference for nonmaximal mixing [23]. Moreover, accelerator data are becoming increasingly competitive with atmospheric data in constraining θ_{23} [19]. Therefore, although we still find (as in previous works [2,4]) that atmospheric data alone prefer $\theta_{23} < \pi/4$, the overall combination with current nonatmospheric data

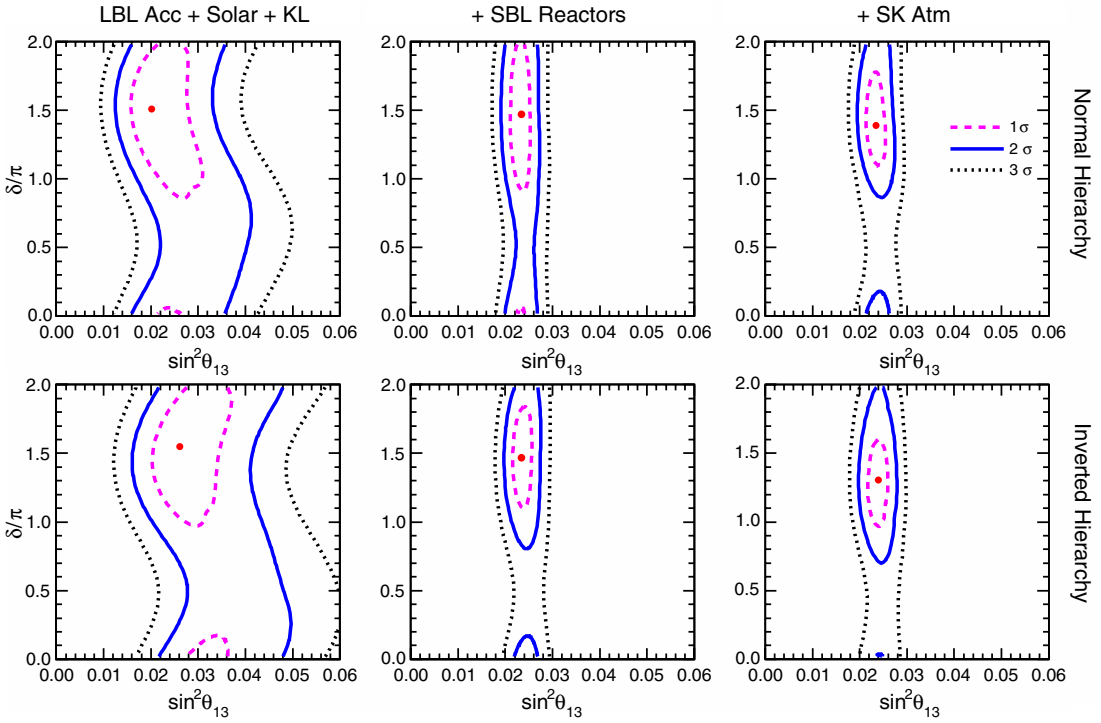

FIG. 6 (color online). As in Fig. 4, but in the plane ($\sin^2\theta_{13}$, δ/π).

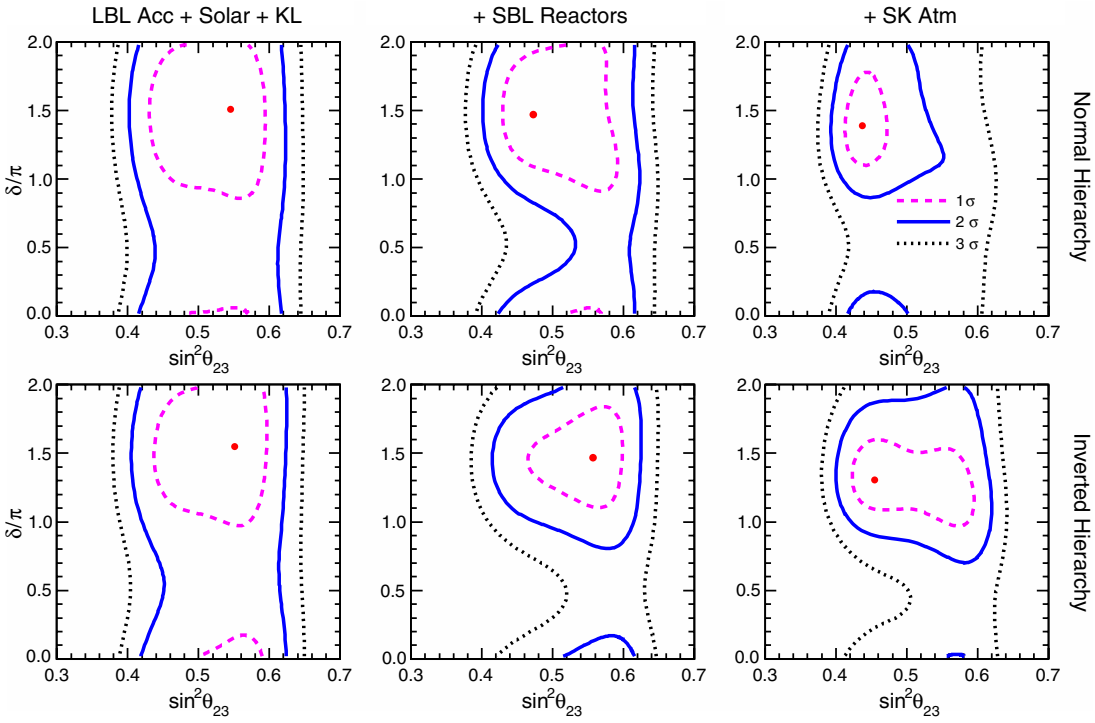

FIG. 7 (color online). As in Fig. 4, but in the plane $(\sin^2\theta_{23}, \delta/\pi)$.

(right panels of Fig. 5) makes this indication less significant than in previous fits (compare, e.g., with Fig. 1 in Ref. [4]), especially in IH, where nonatmospheric data now prefer the opposite case, $\theta_{23} > \pi/4$. The fragility of the θ_{23} octant fit (with and without atmospheric neutrinos) was also noted in the recent analysis [6]. In conclusion, the overall indication for $\theta_{23} < \pi/4$ in both NH and IH (right panels of Fig. 5) is currently weaker than in our previous analysis [4]; in particular, its significance reaches only $\sim 1.6\sigma$ (90% C.L.) in NH, while it is $< 1\sigma$ in IH. Further accelerator neutrino data will become increasingly important in assessing the status of θ_{23} in the near future.

Figure 6 shows the allowed regions in the plane $(\sin^2\theta_{13}, \delta/\pi)$, which is at the focus of current research in neutrino physics. In the left panels, with respect to previous results in the same plane [4], there is now a more marked preference for $\delta \sim 1.5\pi$, where a compromise is reached between the relatively high θ_{13} values preferred by the T2K appearance signal and the relatively low value preferred by solar + KL data. In the middle panel, SBL reactor data strengthen this trend by reducing the covariance between θ_{13} and δ. It is quite clear that we can still learn much from the combination of accelerator and reactor data in the next few years. Finally, the inclusion of SK atmospheric data in the right panels also adds some statistical significance to this trend, with a slight lowering of the best-fit value of δ.

Figure 7 completes our discussion by showing the allowed regions in the plane $(\sin^2\theta_{23}, \delta/\pi)$. The shapes of the allowed regions are rather asymmetrical in the two θ_{23} octants, which are physically inequivalent in the flavor appearance phenomenology of accelerator and atmospheric neutrinos. Therefore, reducing the octant degeneracy will also help, indirectly, our knowledge of δ. Eventually, more subtle covariances may be studied in this plane [37], but we are still far from the required accuracy.

V. SUMMARY AND CONCLUSIONS

In the light of recent new data (circa 2013–2014) coming from reactor and accelerator experiments, and of their interplay with solar and atmospheric data, we have updated the estimated $N\sigma$ ranges of the known 3ν parameters $(\Delta m^2, \delta m^2, \theta_{12}, \theta_{13}, \theta_{23})$, and we have revisited the status of the current unknowns $[\mathrm{sign}(\Delta m^2), \mathrm{sign}(\theta_{23} - \pi/4), \delta]$. The results of the global analysis of all data are shown in Fig. 3 and in Table I, from which one can derive the ranges of the known parameters; in particular, as compared with a previous analysis [4], one can appreciate a significant reduction of the θ_{13} uncertainties and some changes in the $(\Delta m^2, \theta_{23})$ ranges.

We have also discussed in detail the status of the unknown parameters. Concerning the hierarchy $[\mathrm{sign}(\Delta m^2)]$, we still find no appreciable difference between normal and inverted mass ordering. With respect to Ref. [4], we continue to find an overall preference for the first θ_{23} octant, but with a lower statistical significance, which exceeds 1σ only in NH. This feature of the current analysis is mainly due to the persisting preference of (increasingly accurate) T2K disappearance data for nearly maximal mixing [19], as opposed to somewhat different

indications coming from the analysis of MINOS [23] and atmospheric data [4]. Probably the most intriguing feature of the current data analysis is the emergence of an overall preference for nonzero CP violation around $\delta \sim 1.4\pi$ (with $\sin\delta < 0$) at the $\gtrsim 1\sigma$ level, while some ranges with $\sin\delta > 0$ are disfavored at $\gtrsim 2\sigma$.

In order to understand how the various constraints and hints emerge from the analysis, and to appreciate their (in) stability, we have considered increasingly rich data sets, starting from the combination of LBL accelerator plus solar plus KamLAND data, then adding SBL reactor data, and finally including atmospheric data. We have discussed the fit results both on single parameters and on selected couples of correlated parameters. We remark that the θ_{23} octant issue appears somewhat unstable at present, while the hints about δ (despite being still statistically weak) seem to arise from an overall convergence of several pieces of data. Of course, these might just be fluctuations: the search for $[\mathrm{sign}(\Delta m^2), \mathrm{sign}(\theta_{23} - \pi/4), \delta]$is still open to all possible outcomes. In this context, joint 3ν analyses of LBL accelerator data (in both appearance and disappearance modes) and SBL reactor data have the potential to bring interesting new results in the next few years.

AKNOWLEDGMENTS

F. C., G. L. F., E. L., A. M., and D. M. acknowledge support from the Istituto Nazionale di Fisica Nucleare (INFN, Italy) through the "Astroparticle Physics" research project. A. P. acknowledges support from the European Community through a Marie Curie Intra-European Fellowship, Grant No. PIEF-GA-2011-299582 "On the Trails of New Neutrino Properties." He also acknowledges partial support from the European Union FP7 ITN INVISIBLES (Marie Curie Action No. PITN-GA-2011-289442). Preliminary results of this work were presented by E. L. at *NNN13*, the XIV International Workshop on Next-Generation Nucleon Decay and Neutrino Detectors (Kashiwa, Japan, 2013); at *NuPhys 2013*, the Topical Research Meeting on Prospects in Neutrino Physics (London, UK, 2013); and at *ICFA 2014*, the European Meeting of the International Committee for Future Accelerators (Paris, France, 2014).

[1] K. Nakamura, H. Kamano, T.-S. H. Lee, and T. Sato (Particle Data Group), Phys. Rev. D **86**, 010001 (2012).
[2] G. L. Fogli, E. Lisi, A. Marrone, and A. Palazzo, Prog. Part. Nucl. Phys. **57**, 742 (2006).
[3] *Proceedings of Neutrino 2012, the XXV International Conference on Neutrino Physics and Astrophysics* (Kyoto, Japan, 2012), edited by T. Kobayashi, M. Nakahata, and T. Nakaya, *Nucl. Phys. B (Proc. Suppl.)* **235–236** (2013), pp 481.
[4] G. L. Fogli, E. Lisi, A. Marrone, D. Montanino, A. Palazzo, and A. M. Rotunno, Phys. Rev. D **86**, 013012 (2012).
[5] M. C. Gonzalez-Garcia, M. Maltoni, J. Salvado, and T. Schwetz, J. High Energy Phys. 12 (2012) 123.
[6] An updated version of the results in Ref. [5] can be found at the website www.nu-fit.org; see the link therein: "v1.2: Three-neutrino results after the TAUP 2013 Conference".
[7] D. V. Forero, M. Tortola, and J. W. F. Valle, Phys. Rev. D **86**, 073012 (2012).
[8] G. L. Fogli, E. Lisi, A. Marrone, A. Palazzo, and A. M. Rotunno, in *Proceedings of NO-VE 2008, the IV International Workshop on "Neutrino Oscillations in Venice"* (Venice, Italy, 2008), edited by M. Baldo Ceolin (University of Padova, Papergraf Editions, Padova, Italy, 2008), p. 21; also available at neutrino.pd.infn.it/NO-VE2008.
[9] G. L. Fogli, E. Lisi, A. Marrone, A. Palazzo, and A. M. Rotunno, Phys. Rev. Lett. **101**, 141801 (2008).
[10] A. B. Balantekin and D. Yilmaz, J. Phys. G **35**, 075007 (2008).
[11] G. L. Fogli, E. Lisi, A. Marrone, A. Palazzo, and A. M. Rotunno, in *NEUTEL 2009, Proceedings of the 13th International Workshop on Neutrino Telescopes* (Venice, Italy, 2009), published by M. Baldo Ceolin (University of Padova, Papergraf Editions, Padova, Italy), p. 81.
[12] F. P. An *et al.* (Daya-Bay Collaboration), Phys. Rev. Lett. **108**, 171803 (2012).
[13] J. K. Ahn *et al.* (RENO Collaboration), Phys. Rev. Lett. **108**, 191802 (2012).
[14] Y. Abe *et al.* (Double Chooz Collaboration), Phys. Rev. D **86**, 052008 (2012).
[15] F. P. An *et al.* (Daya Bay Collaboration), Phys. Rev. Lett. **112**, 061801 (2014).
[16] H. Seo (the RENO Collaboration), talk at WIN 2013, *XXIV International Workshops on Weak Interactions and Neutrinos* (Natal, Brazil, 2013), hep.if.usp.br/WIN13.
[17] K. Abe *et al.* (T2K Collaboration), Phys. Rev. Lett. **112**, 061802 (2014).
[18] K. Abe *et al.* (T2K Collaboration), Phys. Rev. Lett. **111**, 211803 (2013).
[19] K. Abe *et al.* (T2K Collaboration), arXiv:1403.1532.
[20] P. Adamson *et al.* (MINOS Collaboration), Phys. Rev. Lett. **110**, 171801 (2013).
[21] P. Adamson *et al.* (MINOS Collaboration), Phys. Rev. Lett. **110**, 251801 (2013).
[22] J. Coelho (the MINOS Collaboration), talk at *NuFact 2013, XV International Workshop on Neutrino Factories, Super Beams and Beta Beams* (Beijing, China, 2013); nufact2013.ihep.ac.cn.
[23] P. Adamson *et al.* (MINOS Collaboration), arXiv:1403.0867 [Phys. Rev. Lett. (to be published)].
[24] GLoBES, General Long Baseline Experiment Simulator; www.mpi-hd.mpg.de/~globes.

[25] P. Huber, M. Lindner, and W. Winter, Comput. Phys. Commun. **167**, 195 (2005); P. Huber, J. Kopp, M. Lindner, M. Rolinec, and W. Winter, Comput. Phys. Commun. **177**, 432 (2007).
[26] A. Palazzo, J. High Energy Phys. 10 (2013) 172.
[27] L. K. Pik, Ph.D. thesis, (University of Tokyo, Japan, 2012).
[28] R. Wendell (Super-Kamiokande Collaboration), in *Proceedings of NOW 2012, Neutrino Oscillation Workshop* (Otranto, Italy, 2012), edited by P. Bernardini, G. L. Fogli, and E. Lisi, *Nucl. Phys. B, Proc. Suppl.* **237–238**, 163 (2013).
[29] A. Himmel (the Super-Kamiokande Collaboration), arXiv:1310.6677; to appear in *Proceedings of PPC 2013, 7th International Conference on Interconnection between Particle Physics and Cosmology* (Deadwood, SD, USA, 2013).
[30] E. Kh. Akhmedov, M. Maltoni, and A. Yu. Smirnov, J. High Energy Phys. 06 (2008) 072.
[31] A. B. Balantekin *et al.*, arXiv:1307.7419.
[32] F. Capozzi, E. Lisi, and A. Marrone, Phys. Rev. D **89**, 013001 (2014).
[33] M. Blennow, P. Coloma, P. Huber, and T. Schwetz, J. High Energy Phys. 03 (2014) 028.
[34] G. L. Fogli, E. Lisi, and A. Palazzo, Phys. Rev. D **65**, 073019 (2002).
[35] A. Cervera, A. Donini, M. B. Gavela, J. J. Gomez Cadenas, P. Hernandez, O. Mena, and S. Rigolin, Nucl. Phys. **B579**, 17 (2000); A. Cervera, A. Donini, M. B. Gavela, J. J. Gomez Cadenas, P. Hernandez, O. Mena, and S. Rigolin, Nucl. Phys. **B593**, 731(E) (2001).
[36] M. Freund, Phys. Rev. D **64**, 053003 (2001).
[37] H. Minakata and S. J. Parke, Phys. Rev. D **87**, 113005 (2013).